THE ASTROPHYSICAL JOURNAL, 434:L55–L58, 1994 October 20

THE Θ-z RELATION FOR *HST*[1] BULGES AND DISKS OUT TO $z \simeq 0.8$

STEVEN B. MUTZ,[2] ROGIER A. WINDHORST,[2,3] PAUL C. SCHMIDTKE,[2] AND SEBASTIAN M. PASCARELLE[2]
Department of Physics and Astronomy, Arizona State University, Tempe, AZ 85287-1504
sbm, raw, pcs, smp@cosmos.la.asu.edu

RICHARD E. GRIFFITHS, KAVAN U. RATNATUNGA, STEFANO CASERTANO, AND MYUNGSHIN IM
Johns Hopkins University, Bloomberg Center for Physics and Astronomy, Baltimore, MD 21218-2695
griffith, kavan, stefano, myung@mds.pha.jhu.edu

RICHARD S. ELLIS[2] AND KARL GLAZEBROOK[2]
Institute of Astronomy, Madingley Road, Cambridge CB3 0HA, England, UK
rse, kgb@mail.ast.cam.ac.uk

AND

RICHARD F. GREEN[2] AND VICKI L. SARAJEDINI[2]
National Optical Astronomy Observatories, 950 North Cherry Ave, Tucson, AZ 85725-6732
green, vicki@noao.edu

Received 1994 June 20; accepted 1994 August 1

ABSTRACT

We present *HST* scale lengths and ground-based redshifts for 63 faint field galaxies down to $I \lesssim 21.5$ mag from the Medium-Deep Survey. These have measured redshifts $z \lesssim 0.8$ and *half-light* radii $0''.1 \lesssim r_e$, $r_s \lesssim 5''$. We present the Θ-z relation for $r^{1/4}$-bulges and exponential disks separately for world models with $q_0 = 0.0$–1.0. We show that selection against low surface brightness galaxies in the *HST* images and ground-based spectra is comparable to that in local surveys.

We compare our *HST* disk-dominated galaxies to a *magnitude-limited* subsample of the ESO-Uppsala local spirals. Extrapolating the best-fit local exponential disk scale length ($r_s = 3.5$ kpc for $H_0 = 75$) out to $z = 0.8$, we find a rather symmetrical distribution of *HST* disks around this value. This implies that galaxy disks have been stable since $z \simeq 0.8$. We compare our *HST* bulge-dominated galaxies with $r^{1/4}$-profiles to a *magnitude-limited* subsample of local Seven Samurai ellipticals. The latter have a local best fit $r_e = 5.7$ kpc. Our *HST* bulge sample shows a similar distribution for $z \lesssim 0.8$. Elliptical galaxy scale lengths have thus also remained rather constant since $z \lesssim 0.8$. We set limits to their possible evolution.

Subject headings: cosmology: observations — galaxies: distances and redshifts — galaxies: evolution

1. INTRODUCTION

Until the deployment of *HST* in 1990, it was impossible to accurately determine scale lengths for galaxies with $21 \lesssim V \lesssim 24$ mag with ground-based telescopes, because (1) their median scale length is $\sim 0''.4$ for $V \lesssim 24$ mag (Griffiths et al. 1994a, hereafter G94), and (2) proper sampling of the light profiles requires a resolution $\lesssim 0.5$ times the smallest scale length. The spherical aberration in *HST*'s primary mirror and its impact on the *HST* data reduction have been extensively studied (e.g., Windhorst, Mathis, & Keel 1992, hereafter W92; Windhorst et al. 1994a [hereafter W94a], 1994b [hereafter W94b]; Keel & Windhorst 1993, hereafter KW93) and show that proper deconvolution algorithms are nearly photon preserving and restore the galaxy's morphology and light profiles quite well. The prerefurbished *HST* lowers the limit of the smallest observable scale length to $\sim 0''.2$ FWHM, as indicated by the horizontal dot-dashed lines in Figures 1*a* and 1*b*. Combining *HST* images with ground-based spectroscopy allows us for the first time to extend the optical Θ-z relation of galaxy disks and bulges beyond $z \gtrsim 0.1$–0.2 and to systematically study galaxy scale lengths and their possible evolution with cosmic time, which is the goal of this *Letter*. We use $H_0 = 75$ km s^{-1} Mpc^{-1}.

2. OBSERVATIONS AND DATA PROCESSING

Since 1992 January, the *HST* Medium-Deep Survey (MDS) has used the Wide-Field Camera (WFC) in parallel observing mode to randomly image the sky in the I ($\lambda_{\rm eff} = 8920$ Å) and V (5420 Å) filters. In cycles 1–3, the WFC imaged 97 fields at high Galactic latitude, containing $\sim 17{,}000$ galaxies down to $V \lesssim 24$ mag (G94). Details of the observation and reduction methods can be found in G94, Ratnatunga et al. (1994a), and Windhorst, Franklin, & Neuschaefer (1994).

For most galaxies, we used a maximum-likelihood method to extract quantitative structural parameters (see Ratnatunga, Casertano, & Griffiths 1994, hereafter R94b). Models for each galaxy and the instrumental point-spread function (PSF) of the prerefurbished WFC were constructed for each orbital image (Krist 1992). The model galaxies were convolved with the WFC PSF, and a maximum-likelihood algorithm estimated which model ($r^{1/4}$-bulge or exponential disk, or both, centroid position, sky background, total magnitude, half-light radius

[1] Based on observations with the NASA/ESA *Hubble Space Telescope*, obtained at the Space Telescope Science Institute, which is operated by the Association of Universities for Research in Astronomy, Inc., under NASA contract NAS 5-26555.

[2] Optical observations obtained at the Multiple Mirror Telescope Observatory, a joint facility of the University of Arizona and the Smithsonian Institution, at the 100 inch (du Pont 2.54 m) Telescope of the Observatories of the Carnegie Institution of Washington, at the William Herschel Telescope of the Observatorio del Roque de los Muchachos on La Palma, and at the National Optical Astronomy Observatories, which are operated by the Association of Universities for Research in Astronomy, Inc., under contract with the National Science Foundation.

[3] Alfred P. Sloan Research Fellow.

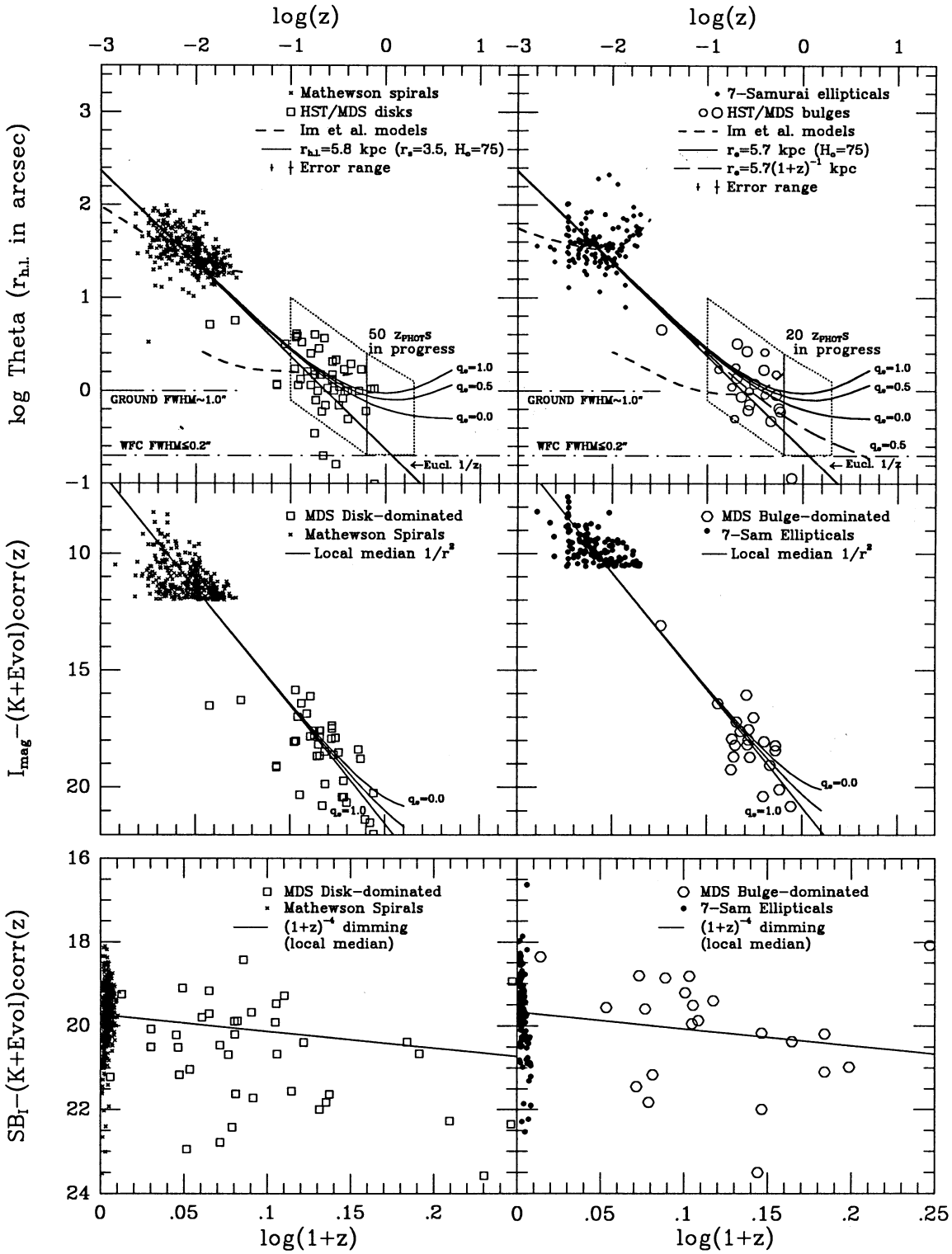

FIG. 1.—(*Upper left*) Scale length Θ vs. redshift z for *HST*/MDS disk-dominated galaxies with spectroscopically measured redshifts. The *magnitude-limited* Mathewson et al. (1992) local spiral subsample is plotted with small crosses; the solid line is their median best fit of r_{hl} = 5.8 kpc, which was extrapolated to higher redshifts for several values of q_0; the Euclidean prediction is also plotted. Dashed lines indicate the no-evolution predictions of Im et al. (1994). (*Upper right*) same as in (*a*), but for *HST*/MDS bulge-dominated galaxies with spectroscopically measured redshifts. The *magnitude-limited* Seven Samurai local elliptical subsample of Burstein et al. (1987) is plotted (*small dots*), as well as its median best fit of r_e = 5.7 kpc. (*Middle left*) *I*-magnitude vs. log z for the same samples as in (*a*). (*Middle right*) Same as in (*c*), but for the same samples as in (*b*). (*Lower left*) Rest frame *I*-band SB vs. log (1 + z) for the same samples as in (*c*). (*Lower right*) Same as in (*e*), but for the same samples as in (*d*). Solid lines indicate the best-fit median through the (K + evolution–corrected) local samples, as discussed in the text.

r_{hl}, axis ratio, and sky position angle) produced the best χ^2 fit to the aberrated data. Throughout, "scalelength" refers to the *semimajor* axis of the ellipse which contains half of the total integrated galaxy flux, i.e., the *half-light* "radius," r_e or r_{hl}, for bulges and disks, respectively. For pure bulges, r_{hl} = de Vaucouleurs r_e; for pure disks $r_{hl} = 1.67 \times r_s$, where r_s is the exponential Freeman scale length. Their deconvolved light profiles and color gradients are discussed by Schmidtke et al. (1994).

We obtained ground-based spectroscopy for 78 faint field galaxies using the Steward Observatory 4.5 m Multiple Mirror Telescope (MMT), the KPNO Mayall 4 m with the CryoCam Spectrograph, the LDSS-2 at the 4.2 m William Herschel Telescope (WHT) at La Palma, and the Carnegie 2.5 m du Pont telescope at Las Campanas Observatory (LCO). These came from 29 MDS images with total integration times between 1200–29,000 s. For the MMT and LCO runs, spectroscopic targets were selected from these 29 *I*-band images as randomly as possible, but working top-down in *I*-band magnitude, so as to have a magnitude-limited subsample at any given time. For the Mayall and WHT runs, multislit masks were prepared for longer integrations and fainter galaxies, but only in 10 MDS fields. We also included seven field galaxies and two weak ratio galaxies from the WFPC images of W94b, which had similar selection criteria.

We were able to secure redshifts for 63 field galaxies in our MDS sample with $I \lesssim 21$ mag. Redshifts ranged from $z = 0.014$ to $z = 0.766$. There were 12 objects in common between the CryoCam and MMT/LCO samples, with a discordant redshift for only one object with very low signal-to-noise ratio (S/N) in both cases (which was discarded pending better spectra).

3. RESULTS: THE Θ-z RELATION

3.1. *Possible Selection Effects*

We should first consider the distribution in luminosity and rest frame SB of the local and the *HST* samples. In Figure 1*c*, we plot the total *I*-band magnitudes versus log *z* for the local spirals from the ESO/Uppsala sample of Mathewson, Ford, & Buchhorn (1992) and for the MDS disk-dominated galaxies with bulge-to-disk ratios (B/D) < 1.0. In Figure 1*d* we plot the total *I*-band magnitudes for the MDS bulge-dominated galaxies (B/D > 1.0) and for the Seven Samurai sample of local elliptical galaxies (Burstein et al. 1987), the latter transformed from their measured *B* magnitudes and the known local correlation between $(B-I)$ and $(B-V)$ (Roberts & Haynes 1994; Bruzual 1983). Despite the limitations discussed below, these are the best local samples available with carefully measured scale lengths. In Figure 1*e* we plot the *rest frame I*-band SB for the Mathewson spiral galaxies and the MDS disks versus log $(1 + z)$, and in Figure 1*f* for the Seven Samurai elliptical galaxies and the MDS bulges. Here we define SB as the *average* surface brightness within the galaxy's half-light radius, as in the local samples. To all samples we applied "*K*-corrections" for both the effects of redshift on a nonevolving spectral energy distribution (SED) and for the expected spectral evolution (Bruzual 1983). Fortunately, Mathewson et al. (1992) give *I*-band magnitudes, in which *K* + evolutionary–corrections are rather small ($\lesssim$0.2 mag) for $z \lesssim 0.8$. Also, internal absorption in *I* is smaller than in *V*. The *I*-band MDS images sample typically rest frame *R*. The *BVRIHK* profiles of the 86 local spirals of de Jong & van der Kruit (1994) are remarkably similar, so that the modest changes of λ_{eff} with redshift should not affect the values of r_{hl} significantly. Because the central bulge SB of B/D > 1 galaxies is several magnitudes above their central disk SB, their bulge r_{hl} is not significantly affected by the disk component in our fitting algorithm, so that we may compare the bulge r_{hl} of B/D > 1 spirals to ellipticals.

The lines in Figures 1*c* and 1*d* have slope 5 and are drawn at the *median* total magnitude of the local samples. Figures 1*c* and 1*d* show that the MDS disks and bulges have about the same total absolute magnitude distribution as the corresponding local samples, after proper *K* + evolutionary corrections, showing that selection biases by the *HST* images and/or ground-based spectroscopy against low-luminosity galaxies operate similarly as in the local samples.

The lines in Figures 1*e* and 1*f* indicate the $(1 + z)^{-4}$ SB-dimming relation at the median SB of the local samples. Figure 1*e* shows that MDS disk galaxies have somewhat lower rest frame SB than the extrapolated local median (25 objects below and 14 above the line). This may arise because the Mathewson sample is biased against Irr galaxies (and S0/Sa disks). Figure 1*f* shows that MDS bulges have marginally higher rest frame SB than the extrapolated local median (eight objects below and 14 above the line). Our orbital *HST* images, as well as the successful spectroscopic redshift measurements, may select against faint low-SB galaxies and thus affect our sample completeness for $z \gtrsim 0.2$–0.3. We therefore made an a priori attempt to get the best possible complete *HST* sample by *convolving* the read noise–limited MDS WFC images to the known median galaxy scale length for $V \lesssim 24$ mag ($\simeq$0".4, G94, R94b) and then running the FOCAS object finder adapted to *HST* (see Neuschaefer, Griffiths, & Ratnatunga 1994 for details). This procedure did *not* yield a significant number of additional low-SB galaxies, consistent with Burkey et al. (1994), who similarly found *I*-band galaxy counts consistent with ground-based for $I \lesssim 22$ mag. The presence of *HST* disks and bulges in Figures 1*e* and 1*f* with rest frame SB as low as the *lowest* SB seen in the *local* samples shows that the *HST* images and ground-based spectra do *not* produce unreasonably small fractions of low-SB galaxies with $z \lesssim 0.3$. In conclusion, our sample apparently picks up galaxies of similar luminosity and similar, if not *lower*, SB as the local samples, so that selection biases in the high- and low-redshift samples are comparable. While Figures 1*c*–1*f* show that the high- and low-redshift disk and bulge-dominated samples select to first-order galaxies of similar luminosity and rest frame SB, we caution the reader that cosmological effects, evolution, and selection effects are difficult to separate.

3.2. *Discussion of Results*

Figure 1*a* shows the Θ-*z* relation for *HST disk-dominated* galaxies out to $z \lesssim 0.8$, compared to the Mathewson sample of local spirals. The Θ-*z* relation of the latter is complicated by its diameter-limited selection. We therefore cut off this sample severely at $I \lesssim 12.0$ mag (see Fig. 1*c*) to construct a magnitude-limited subsample (we could find a uniform V/V_{max} only for $I \lesssim 12.0$ mag, but not for fainter magnitude-limited subsamples; we found these biases in the RC3 to be far worse). This procedure gives the Mathewson sample reasonable completeness in diameter, but only for $z \lesssim 0.01$. The best-fit scale length of the *magnitude-limited* Mathewson subsample is r_{hl} = 5.8 kpc for $z \lesssim 0.01$ (or Freeman r_s = 3.5 kpc). Figure 1*a* shows the Friedmann models for $r_{hl} = 5.8$ kpc, $H_0 = 75$ km s^{-1} Mpc^{-1}, and $q_0 = 0.0$, 0.5, and 1.0, as well as the Euclidean relation.

Figure 1*b* shows the Θ-z relation for *HST bulge-dominated* galaxies out to $z \lesssim 0.8$, compared to the Seven Samurai local elliptical galaxies. Large filled circles indicate *HST* galaxies with pure, or nearly pure, bulges (B/D $\gtrsim$ 3), and smaller filled circles indicate *HST* bulge-dominated galaxies with a substantial disk component (1 $\lesssim$ B/D $\leq$ 3). We also applied a severe magnitude limit ($B \lesssim 12.3$, $I \lesssim 10.3$ mag) to the Seven Samurai sample to remove the effects from its additional sample of cluster ellipticals. Its V/V_{max} is now also uniform. Figure 1*b* shows the same world models as in Figure 1*a*, but for the best-fit *local* scale length $r_e = 5.7$ kpc to the *magnitude-limited* Seven Samurai sample. The leftmost dotted box in Figures 1*a* and 1*b* delineates the range of observed scale lengths in the MDS field of G94 and R94b down to $I \lesssim 22$ mag (for which redshifts are not available as yet), as well as the redshift range expected for their sample. Our sample roughly fills this box, but also covers more MDS fields, and thus yields some more lower redshift galaxies. At $I \sim 22$ mag, the median redshift is expected to be $z \gtrsim 0.6$ from measured I-band redshift distributions (for $I \lesssim 22$ mag; as summarized by Burkey et al. 1994). For *HST*/MDS galaxies of $I \sim 23$ mag, we are not likely to get spectroscopic redshifts and are in the process of constraining their redshift range from deep seven-band *BRVIJHK* photometry (as indicated by the right dotted box in Figs. 1*a* and 1*b*; see Mutz et al. 1994).

In Figures 1*a* and 1*b* we also show the galaxy evolution models of Im et al. (1994), who predict the observed Θ-z relation, using the known selection criteria of the *magnitude-limited* local subsamples, as well as the known strong positive correlation between absolute luminosity and physical scale length (see, e.g., Binggeli, Sandage, & Tarenghi 1984). Im's models predict that even a local magnitude-limited sample does not follow the -1 slope expected for a Θ-z relation (because of the strong r_{hl}-M_B relation, in combination with the magnitude-limited nature of the samples). Similar predictions were made for *HST* bulges and disks, assuming an r_{hl}-M_B relation that did not evolve with cosmic time. The distribution of *HST* MDS disks in Figure 1*a* is nearly asymmetrical around the extrapolated Friedmann models, as well as around the Im et al. (1994) models. The distribution of *HST* bulges in Figure 1*b* shows similar behavior.

We calculated the skewness of the *HST* MDS disk and bulge r_{hl}'s with respect to the extrapolated best fits to the local samples and found that disk and bulge scale lengths have remained roughly constant with cosmic time since $z \lesssim 0.8$.

4. DISCUSSION AND CONCLUSIONS

We presented the Θ-z relation for 63 *HST* bulges and disks out to $z \lesssim 0.8$, based on systematic WF/PC imaging and ground-based spectroscopy of faint field galaxies from the *HST* MDS. Our main conclusions are that (1) selection effects against low-SB galaxies (either in the *HST* images or in succesful ground-based spectra) are not larger than in the best available local comparison samples, and (2) the physical scale lengths of *HST* galaxy disks and bulges have not evolved drastically since $z \lesssim 0.8$. Given their likely dynamical collapse time, they thus likely have been stable since $z \lesssim 1$.

We note that the *entire* Mathewson and Seven Samurai samples—which are *not* magnitude-limited and *in*complete (and therefore not plotted)—contain a population of galaxies with rather small scale lengths. The question arises if the fraction of low-luminosity disks (and bulges?) increases toward larger redshifts. To answer this question, we also need improved *local* surveys, as these objects are poorly represented in *complete* local surveys.

It is possible that some evolution in elliptical galaxy scale lengths may be induced by processes such as merging or dynamical evolution. Recent *HST* work by Burkey et al. (1994) provides hints that the field galaxy merger rate may have increased toward larger redshifts by about $\propto(1+z)^{+3}$. In the simplest scenario, the scale lengths of the putative merger products—elliptical galaxies—may have grown as $\propto$(the resulting merger volume)$^{1/3}$. The resulting elliptical scale length evolution would be $\propto(1+z)^{-1}$ kpc. The dashed line in Figure 1*b* represents this relation, but only for $q_0 = 0.5$. Our distribution of *HST* bulge scale lengths is consistent with this relation, although it does not require size evolution of this strength due to the limited statistics. However, our current data rules out size evolution stronger than $\propto(1+z)^{-1}$. Merging and dynamical evolution are more likely to cause scale length evolution in ellipticals than in spirals [although for both it must be weaker than $\propto(1+z)^{-1}$]. If larger *HST* samples with (larger) redshifts, and better local samples, can be defined, it may ultimately be possible to constrain q_0 from *HST* scale lengths—with spiral disks as the best candidate rigid rods.

This work was supported by NASA/*HST* grants GO-2684-0*-87A, 91A, 92A from STScI, which is operated by AURA, Inc., under NASA contract NAS 5-26555. We thank Barbara Franklin and Eric Ostrander for their help with the WFPC Pipeline, John Huchra for help with interpretation of the spectra, and Dave Burstein and Alan Sandage for useful discussions.

REFERENCES

Binggeli, B., Sandage, A., & Tarenghi, M. 1984, AJ, 89, 64
Bruzual, A. G. 1983, ApJ, 273, 105
Burkey, J. M., Keel, W. C., Windhorst, R. A., & Franklin, B. E. 1994, ApJ, 429, L13
Burstein, D., et al. 1987, ApJS, 64, 601
de Jong, R. S., & van der Kruit, P. C. 1994, A&AS, in press
Griffiths, R. E., et al. 1994a, ApJ, in press (G94)
———. 1994b, ApJ, in press
Im, M., Casertano, S., Griffiths, R. E., & Ratnatunga, K. U. 1994, ApJ, submitted
Keel, W. C., & Windhorst, R. A. 1993, AJ, 106, 455 (KW93)
Krist, J. 1992, The Tiny TIM User's Manual, Version 2.1 (Baltimore: STScI)
Mathewson, D. S., Ford, V. L., & Buchhorn, M. 1992, ApJS, 81, 413
Mutz, S. B., et al. 1994, in preparation
Neuschaefer, L. W., Griffiths, R. E., Ratnatunga, K. U., & Valdes, F. 1994, AJ, submitted
Ratnatunga, K. U., et al. 1994a, AJ, submitted
Ratnatunga, K. U., Casertano, S., & Griffiths, R. E. 1994b, in preparation (R94b)
Roberts, M. S., & Haynes, M. P. 1994, ARA&A, in press
Schmidtke, P. C., et al. 1994, in preparation
Windhorst, R. A., Mathis, D. F., & Keel, W. C. 1992, ApJ, 400, L1 (W92)
Windhorst, R. A., et al. 1994a, AJ, 107, 930 (W94a)
———. 1994b, ApJ, in press (W94b)
Windhorst, R. A., Franklin, B. E., & Neuschaefer, L. W. 1994, PASP, 106, 798